Rotational surfaces with prescribed mean curvature in $\mathbb{H}^2 \times \mathbb{R}$

Antonio Bueno[†], Irene Ortiz[‡]

[†]Departamento de Ciencias, Centro Universitario de la Defensa de San Javier, E-30729 Santiago de la Ribera, Spain.
E-mail address: antonio.bueno@cud.upct.es

[‡]Departamento de Ciencias, Centro Universitario de la Defensa de San Javier, E-30729 Santiago de la Ribera, Spain.
E-mail address: irene.ortiz@cud.upct.es

Abstract

In this paper we study rotational surfaces in the space $\mathbb{H}^2 \times \mathbb{R}$ whose mean curvature is given as a prescribed function of their angle function. These surfaces generalize, among others, the ones of constant mean curvature and the translating solitons of the mean curvature flow. Using a phase plane analysis we construct entire rotational graphs, catenoid-type surfaces, and exhibit a classification result when the prescribed function is linear.

1 Introduction

Let us consider a function $\mathcal{H} \in C^1(\mathbb{S}^2)$. An oriented surface Σ immersed into $\mathbb{R}^3$ is said to be a surface with *prescribed mean curvature* $\mathcal{H}$ if its mean curvature function H_Σ satisfies

$$H_\Sigma(p) = \mathcal{H}(N_p) \tag{1.1}$$

for every point $p \in \Sigma$, where N denotes the *Gauss map* of Σ. For short, we say that Σ is an *$\mathcal{H}$-surface*. Let us observe that when the function $\mathcal{H}$ is chosen as a constant H_0, the surfaces defined by Equation (1.1) are just the surfaces with constant mean curvature (CMC) equal to H_0.

The definition of this class of immersed surfaces has its origins on the famous Christoffel and Minkowski problems for ovaloids [Chr, Min]. The existence of prescribed mean curvature ovaloids was studied, among others, by Alexandrov, Pogorelov and Guan-Guan [Ale, Pog, GuGu], while the uniqueness in the Hopf sense has been recently achieved by Gálvez and Mira [GaMi1]. In this fashion, the first author jointly with Gálvez and Mira started to develop the *global theory of surfaces with prescribed mean curvature in* $\mathbb{R}^3$, taking as motivation the fruitful theory of CMC surfaces, see [BGM1, BGM2]. The first author also proved the existence and uniqueness to the Björling problem [Bue3] and obtained half space theorems for $\mathcal{H}$-surfaces [Bue4].

A relevant case of $\mathcal{H}$-surfaces appears when the function $\mathcal{H}$ depends only on the height of the sphere, i.e., if there exists a one dimensional function $\mathfrak{h} \in C^1([-1,1])$ such that $\mathcal{H}(x) = \mathfrak{h}(\langle x, e_3\rangle)$ for every $x \in \mathbb{S}^2$. In this case, $\mathcal{H}$ is called *rotationally symmetric* and Equation (1.1) reads as

$$H_\Sigma(p) = \mathfrak{h}(\langle N_p, e_3\rangle) = \mathfrak{h}(\nu(p)), \tag{1.2}$$

Mathematics Subject Classification: 53A10, 53C42, 34C05, 34C40.
Keywords: Prescribed mean curvature surface, non-linear autonomous system, phase plane analysis.

for every point $p \in \Sigma$, where $\nu(p) := \langle N_p, e_3 \rangle$ is the so-called *angle function* of Σ. In this setting, the authors have obtained a classification result for rotational $\mathcal{H}$-hypersurfaces in $\mathbb{R}^{n+1}$ satisfying (1.2), whose prescribed function $\mathfrak{h}$ is *linear*, i.e. $\mathfrak{h}(y) = ay + \lambda,\ a, \lambda \in \mathbb{R}$, see [BuOr].

Note that for defining Equation (1.2) we only need to measure the projection of a unit normal vector field onto a Killing vector field. Consequently, surfaces obeying (1.2) can be also defined in the product spaces $\mathbb{M}^2 \times \mathbb{R}$, where $\mathbb{M}^2$ is a complete surface, as follows:

Definition 1.1 *Let $\mathfrak{h}$ be a C^1 function on $[-1, 1]$. An oriented surface Σ immersed in $\mathbb{M}^2 \times \mathbb{R}$ has* prescribed mean curvature $\mathfrak{h}$ *if its mean curvature function H_Σ satisfies*

$$H_\Sigma(p) = \mathfrak{h}(\langle \eta_p, \partial_z \rangle), \tag{1.3}$$

for every point $p \in \Sigma$, where η is a unit normal vector field on Σ and ∂_z is the unit vertical Killing vector field on $\mathbb{M}^2 \times \mathbb{R}$.

Again, note that $\nu(p) := \langle \eta_p, \partial_z \rangle$ is the angle function of Σ. In analogy with the Euclidean case, we will simply say that Σ is an $\mathfrak{h}$-*surface*.

Observe that if $\mathfrak{h}$ is a constant function, we recover the theory of CMC surfaces in $\mathbb{M}^2 \times \mathbb{R}$, which experimented an extraordinary development since Abresch and Rosenberg [AbRo] defined a *holomorphic quadratic differential* on them, that vanishes on rotational examples. This milestone began the research of several properties of CMC surfaces in the product spaces, among which we highlight the study of invariant (including rotationally invariant) CMC surfaces in $\mathbb{H}^2 \times \mathbb{R}$ [BeEa, Oni].

Further results have been obtained for $\mathfrak{h}$-surfaces for rather choices of the prescribed function. If $\mathfrak{h}(y) = y$, the $\mathfrak{h}$-surfaces arising are the translating solitons of the mean curvature flow, see [Bue1, Bue2, LiMa]. At this point, we remark that invariant translators have been classified in other Thurston's geometries [Pip1, Pip2]. For a general function $\mathfrak{h} \in C^1([-1, 1])$ under necessary and sufficient hypothesis, the first author obtained a Delaunay-type classification result in $\mathbb{M}^2 \times \mathbb{R}$ [Bue5], and a structure result for properly embedded $\mathfrak{h}$-surfaces in $\mathbb{H}^2 \times \mathbb{R}$ [Bue6].

Inspired by the results obtained for CMC and minimal surfaces, for translators and for $\mathcal{H}$-surfaces in $\mathbb{R}^3$ and $\mathbb{H}^2 \times \mathbb{R}$, the purpose of this paper is to further investigate the theory of surfaces satisfying (1.3) in the product space $\mathbb{H}^2 \times \mathbb{R}$. Specifically, we focus on the study of rotational $\mathfrak{h}$-surfaces, constructing new examples and providing a classification result for the particular case that $\mathfrak{h}$ is linear.

The rest of the introduction is devoted to detail the organization of the paper and highlight some of the main results.

In Section 2 we deduce the formulae that the profile curve of a rotational $\mathfrak{h}$-surface in $\mathbb{H}^2 \times \mathbb{R}$ satisfy. The resulting ODE will be treated as a non-linear autonomous system, and its qualitative study will be carried out by developing a phase plane analysis. From the previous work [BGM2] we compile the main features of the phase plane adapted to the space $\mathbb{H}^2 \times \mathbb{R}$. In Corollary 2.5 we prove the existence of two unique rotational $\mathfrak{h}$-surfaces, Σ_+ and Σ_-, intersecting orthogonally the axis of rotation with unit normal $\pm\partial_z$, respectively.

In Section 3 we prove in Proposition 3.1 the existence of entire, strictly convex $\mathfrak{h}$-graphs, called $\mathfrak{h}$-bowls in analogy with translating solitons. In Proposition 3.2 we construct properly embedded $\mathfrak{h}$-annuli, called $\mathfrak{h}$-catenoids for their resemblance to the usual minimal catenoids in $\mathbb{R}^3$ and $\mathbb{H}^2\times\mathbb{R}$.

In Section 4 we focus on $\mathfrak{h}_\lambda$-surfaces, which are defined to be those whose prescribed function is linear, i.e. $\mathfrak{h}_\lambda(y) := ay+\lambda,\ a,\lambda\in\mathbb{R}$. The relevance of $\mathfrak{h}_\lambda$-surfaces is that they satisfy certain characterizations that are closely related with the theory of manifolds with density. For instance, $\mathfrak{h}_\lambda$-surfaces have *constant weighted mean curvature* equal to λ with respect to the density e^{ϕ}, where $\phi(x) = a\langle x,\partial_z\rangle,\ \forall x\in\mathbb{H}^2\times\mathbb{R}$. In particular, if $\lambda=0$ we recover the fact that translating solitons are weighted minimal as pointed out by Ilmanen [Ilm]. Also, $\mathfrak{h}_\lambda$-surfaces are critical points for the weighted area functional, under compactly supported variations preserving the weighted volume (see [BCMR] and [BuOr]).

In this section we obtain our two main results in which we achieve a classification of complete rotational $\mathfrak{h}_\lambda$-surfaces in $\mathbb{H}^2\times\mathbb{R}$. First, we prove that we can reduce to study the case $\mathfrak{h}_\lambda(y) = y+\lambda,\ \lambda>0$. If such $\mathfrak{h}_\lambda$-surfaces intersect the axis of rotation we get:

Theorem 1.2 *Let be Σ_+ and Σ_- the complete, rotational $\mathfrak{h}_\lambda$-surfaces in $\mathbb{H}^2\times\mathbb{R}$ intersecting the rotation axis with upwards and downwards orientation respectively. Then:*

1. *For $\lambda>1/2$, Σ_+ is properly embedded, simply connected and converges to the flat CMC cylinder C_λ of radius $\operatorname{arg\,tanh}\left(\frac{1}{2\lambda}\right)$. Moreover:*
   - 1.1. *If $\lambda>\sqrt{2}/2$, Σ_+ intersects C_λ infinitely many times.*
   - 1.2. *If $\lambda=\sqrt{2}/2$, Σ_+ intersects C_λ a finite number of times and is a graph outside a compact set.*
   - 1.3. *If $\lambda<\sqrt{2}/2$, Σ_+ is a strictly convex graph over the disk in $\mathbb{H}^2$ of radius $\operatorname{arg\,tanh}\left(\frac{1}{2\lambda}\right)$.*
2. *For $\lambda\leq 1/2$, Σ_+ is an entire, strictly convex graph.*
3. *For $\lambda>\sqrt{5}/2$, Σ_- is properly immersed (with infinitely many self-intersections), simply connected and has unbounded distance to the rotation axis.*
4. *For $\lambda\leq\sqrt{5}/2$, Σ_- is an entire graph. Moreover, if $\lambda=1$, Σ_- is a horizontal plane (hence minimal and flat), and if $\lambda\neq 1$, Σ_- has positive Gauss-Kronecker curvature.*

For rotational $\mathfrak{h}_\lambda$-surfaces in $\mathbb{H}^2\times\mathbb{R}$ non-intersecting the axis of rotation, we prove the following:

Theorem 1.3 *Let Σ be a complete, rotational $\mathfrak{h}_\lambda$-surface in $\mathbb{H}^2\times\mathbb{R}$ non-intersecting the rotation axis. Then, Σ is properly immersed and diffeomorphic to $\mathbb{S}^1\times\mathbb{R}$. Moreover,*

1. *If $\lambda>1/2$, then:*
   - 1.1. *either Σ is the CMC cylinder C_λ of radius $\operatorname{arg\,tanh}\left(\frac{1}{2\lambda}\right)$, or*
   - 1.2. *one end converges to C_λ with the same asymptotic behavior as in item 1 in Theorem 1.2, and:*

a) If $\lambda > \sqrt{5}/2$, the other end of Σ has unbounded distance to the rotation axis and self-intersects infinitely many times.

b) If $\lambda \leq \sqrt{5}/2$, the other end is a graph outside a compact set.

2. If $\lambda \leq 1/2$, then both ends are graphs outside compact sets.

2 A phase plane analysis of rotational $\mathfrak{h}$-surfaces in $\mathbb{H}^2 \times \mathbb{R}$

In the development of this section, we regard $\mathbb{H}^2 \times \mathbb{R}$ as a submanifold of $\mathbb{R}^3_1 \times \mathbb{R}$ endowed with the metric $+,+,-,+$. Consider a regular curve parametrized by arc-length $\alpha(s) = (x_1(s), 0, x_3(s), z(s)) \subset \mathbb{H}^2 \times \mathbb{R}$, $x_1(s) > 0$, $s \in I \subset \mathbb{R}$, contained in a vertical plane passing through the point $(0,0,1,0)$, and rotate it around the vertical axis $\{(0,0,1)\} \times \mathbb{R}$. Since $x_1^2(s) - x_3^2(s) = -1$, there exists $x(s) > 0$ such that

$$\alpha(s) = (\sinh(x(s)), 0, \cosh(x(s)), z(s)).$$

For saving notation, we will simply denote $\alpha(s)$ by $(x(s), z(s))$. Now, note that the image of $\alpha(s)$ under this 1-parameter group of rotations generates an immersed, rotational surface Σ in $\mathbb{H}^2 \times \mathbb{R}$ parametrized by

$$\psi(s,\theta) = (\sinh(x(s))\cos\theta, \sinh(x(s))\sin\theta, \cosh(x(s)), z(s)) : I \times (0, 2\pi) \to \mathbb{H}^2 \times \mathbb{R}, \tag{2.1}$$

whose angle function at each point $\psi(s,\theta)$ is given by $\nu(\psi(s,\theta)) = x'(s)$, $\forall s \in I$. Moreover, the principal curvatures on Σ are

$$\kappa_1 = \kappa_\alpha = x'z'' - x''z', \qquad \kappa_2 = \frac{z'}{\tanh x}, \tag{2.2}$$

where κ_α stands for the geodesic curvature of the profile curve $\alpha(s)$. Thus, the mean curvature of Σ is easily related to the coordinates of $\alpha(s)$ and bearing in mind that $x'^2 + z'^2 = 1$, we get that the function x is a solution of the autonomous second order ODE

$$x'' = \frac{1 - x'^2}{\tanh x} - 2\varepsilon H_\Sigma \sqrt{1 - x'^2}, \qquad \varepsilon = \operatorname{sign}(z'), \tag{2.3}$$

on every subinterval $J \subset I$ where $z'(s) \neq 0$ for all $s \in J$.

Now, assume that Σ is an $\mathfrak{h}$-surface for some $\mathfrak{h} \in C^1([-1,1])$, that is, by using (1.3) we get $H_\Sigma(\psi(s,\theta)) = \mathfrak{h}(x'(s))$. Hence, after the change $y = x'$, we can rewrite (2.3) as the following autonomous ODE system

$$\begin{pmatrix} x \\ y \end{pmatrix}' = \begin{pmatrix} y \\ \dfrac{1-y^2}{\tanh x} - 2\varepsilon\mathfrak{h}(y)\sqrt{1-y^2} \end{pmatrix} =: F_\varepsilon(x,y). \tag{2.4}$$

At this point, we study this system by using a phase plane analysis as the first author did in [BGM2]. Specifically, the *phase plane* of (2.4) is defined as the half-strip $\Theta_\varepsilon := (0,\infty) \times (-1,1)$, with coordinates (x,y) denoting, respectively, the distance to the rotation axis and the angle function of Σ. The solutions $\gamma(s) = (x(s), y(s))$ of system (2.4) are called *orbits*, and the *equilibrium points* are the points $e_0^\varepsilon = (x_0^\varepsilon, y_0^\varepsilon) \in \Theta_\varepsilon$ such that $F_\varepsilon(x_0^\varepsilon, y_0^\varepsilon) = 0$, which must lie in the axis $y = 0$ according to system (2.4).

Next, we compile some features that can be derived from the study of the phase plane.

Lemma 2.1 *In the above conditions, the following properties hold:*

1. *If $\varepsilon\mathfrak{h}(0) > 1/2$, there is a unique equilibrium $e_0^\varepsilon = (x_0^\varepsilon, 0)$ of (2.4) in Θ_ε given by*

$$x_0^\varepsilon = \operatorname{arctanh}\left(\frac{1}{2\varepsilon\mathfrak{h}(0)}\right).$$

   This equilibrium generates the right circular cylinder $\mathbb{S}^1(x_0^\varepsilon)\times\mathbb{R}$ of constant mean curvature $\mathfrak{h}(0)$ and vertical rulings.

2. *The Cauchy problem associated to (2.4) for the initial condition $(x_0, y_0) \in \Theta_\varepsilon$ has local existence and uniqueness. Thus, the orbits provide a foliation by regular C^1 curves of Θ_ε (or of $\Theta_\varepsilon - \{e_0^\varepsilon\}$, in case some e_0^ε exists).*

3. *The instants $s_0 \in J$ such that $\kappa_\alpha(s_0) = 0$ are the ones for which $x''(s_0) = y'(s_0) = 0$, i.e. those such that $(x(s_0), y(s_0)) \in \Gamma_\varepsilon := \Theta_\varepsilon \cap \{x = \Gamma_\varepsilon(y)\}$, where*

$$\Gamma_\varepsilon(y) = \operatorname{arctanh}\left(\frac{\sqrt{1-y^2}}{2\varepsilon\mathfrak{h}(y)}\right). \tag{2.5}$$

   Moreover, the curve Γ_ε is empty when $\varepsilon\mathfrak{h}(y) \le 0$.

4. *The axis $y = 0$ and the curve Γ_ε divide Θ_ε into connected components, called monotonicity regions, where the coordinates $x(s)$ and $y(s)$ of every orbit are strictly monotonous. Moreover, at each of these regions, we have*

$$\operatorname{sign}(\kappa_1) = \operatorname{sign}(-\varepsilon y'(s)), \quad \operatorname{sign}(\kappa_2) = \operatorname{sign}(\varepsilon). \tag{2.6}$$

Let us focus now on the behavior of the orbits of system (2.4) in more detail. Firstly, note that we can view such orbits as vertical graphs $y = y(x)$ where $y \neq 0$ (i.e. where $x' \neq 0$), so the chain rule yields

$$y'(x)y(x) = \frac{dy}{dx}\frac{dx}{ds} = \frac{dy}{ds} = y'(s) = \frac{1-y^2}{\tanh x} - 2\varepsilon\mathfrak{h}(y)\sqrt{1-y^2}. \tag{2.7}$$

Since at each monotonicity region the sign of the quantity $y(x)y'(x)$ is constant, the behavior of the orbit passing through some $(x_0, y_0) \in \Theta_\varepsilon$ is determined by the signs of y_0 and $\Gamma_\varepsilon(y_0) - x_0$ (whenever $\Gamma_\varepsilon(y_0)$ exists). We detail it next:

Lemma 2.2 *In the above conditions, the behavior of the orbit of (2.4) passing through a given point $(x_0, y_0) \in \Theta_\varepsilon$ such that $\Gamma_\varepsilon(y_0)$ exists is described as follows:*

1. *If $x_0 > \Gamma_\varepsilon(y_0)$ (resp. $x_0 < \Gamma_\varepsilon(y_0)$) and $y_0 > 0$, then $y(x)$ is strictly decreasing (resp. increasing) at x_0.*

2. *If $x_0 > \Gamma_\varepsilon(y_0)$ (resp. $x_0 < \Gamma_\varepsilon(y_0)$) and $y_0 < 0$, then $y(x)$ is strictly increasing (resp. decreasing) at x_0.*

3. *If $y_0 = 0$, then the orbit passing through $(x_0, 0)$ is orthogonal to the x axis.*

4. If $x_0 = \Gamma_\varepsilon(y_0)$, then $y'(x_0) = 0$ and $y(x)$ has a local extremum at x_0.

The following result discusses how an orbit $\gamma(s) = (x(s), y(s)) \in \Theta_\varepsilon$ behaves when $x(s) \to \infty$.

Proposition 2.3 *Let $\gamma(s) = (x(s), y(s))$ be an orbit in Θ_ε such that $(x(s), y(s)) \to (\infty, y_0)$, with $y_0 \in (-1, 1)$. Then, $2\varepsilon\mathfrak{h}(y_0) = \sqrt{1 - y_0^2}$.*

Proof: Suppose that $\gamma(s) \in \Theta_\varepsilon$ satisfies $x(s) \to \infty$ and $y(s) \to y_0 \in (-1, 1)$. In particular, $s \to \pm\infty$, hence we assume without losing generality that $s \to \infty$. Then, there exists $s_0 \in \mathbb{R}$ such that for every $s > s_0$, $\gamma(s)$ is strictly contained in some monotonicity region and so does not intersect the axis $y = 0$. Thus, $\gamma(s)$ can be written as a vertical graph $y = y(x)$ satisfying $y(x) \to y_0$ and $y'(x) \to 0$ as $x \to \infty$, and substituting into Equation (2.7) we get

$$1 - y_0^2 - 2\varepsilon\mathfrak{h}(y_0)\sqrt{1 - y_0^2} = 0$$

concluding the result. □

Additionally, we highlight that the possible endpoints of an orbit are restricted as shown in [BGM2, Theorem 4.1, pp. 13-14].

Lemma 2.4 *No orbit in Θ_ε can converge to some point of the form $(0, y)$ with $|y| < 1$.*

From this result, we conclude that in case that an orbit converges to the axis $x = 0$, it must do it to the points $(0, \pm 1)$. However, we point out that the existence of an orbit with endpoint at $(0, \pm 1)$ can not be guaranteed by solving the Cauchy problem since system (2.4) has a singularity at the points with $x_0 = 0$. In this case, we can ensure the existence of such an orbit by using the work of Gálvez and Mira [GaMi2] in which they solved the Dirichlet problem for radial solutions of an arbitrary *fully nonlinear elliptic PDE*. Therefore, it is ensured the existence of rotational $\mathfrak{h}$-surfaces in $\mathbb{H}^2 \times \mathbb{R}$ intersecting the rotation axis in an orthogonal way (see Section 3 in [Bue5] for further details). Furthermore, this fact derives the following result in the phase plane Θ_ε.

Corollary 2.5 *Let be $\varepsilon, \delta \in \{-1, 1\}$ such that $\varepsilon\mathfrak{h}(\delta) > 0$ and denote $\sigma = \operatorname{sign}(\delta)$. Then, there exists a unique orbit γ_σ in Θ_ε that has $(0, \delta) \in \overline{\Theta_\varepsilon}$ as an endpoint. There is no such an orbit in $\Theta_{-\varepsilon}$.*

The unique rotational $\mathfrak{h}$-surface associated to the orbit γ_σ, that intersects orthogonally the axis of rotation at some point having unit normal $\delta\partial_z$, will be denoted by Σ_σ.

3 Existence of $\mathfrak{h}$-bowls and $\mathfrak{h}$-catenoids in $\mathbb{H}^2 \times \mathbb{R}$

This section is devoted to construct examples of properly embedded rotational $\mathfrak{h}$-surfaces in $\mathbb{H}^2 \times \mathbb{R}$, under some additional assumptions over the function $\mathfrak{h} \in C^1([-1, 1])$. For this purpose, we follow the ideas compiled in Section 3 in [BGM2].

First, recall that in $\mathbb{H}^2 \times \mathbb{R}$ there exists an entire graph with CMC equal to $H_0 \in \mathbb{R}$ if and only if $|H_0| \leq 1/2$. In addition, there exists a sphere with CMC equal to H_0 if and only if $|H_0| > 1/2$.

Regarding $\mathfrak{h}$-surfaces, a necessary and sufficient condition to ensure the existence of a rotational $\mathfrak{h}$-sphere in $\mathbb{H}^2\times\mathbb{R}$ is that $\mathfrak{h}$ must be even and satisfy

$$2|\mathfrak{h}(y)| > \sqrt{1-y^2} \tag{3.1}$$

for every $y\in[-1,1]$, see Proposition 3.7 and Theorem 4.1 in [Bue5].

The next result shows the existence of entire, vertical, rotational $\mathfrak{h}$-graphs in $\mathbb{H}^2\times\mathbb{R}$ by assuming that equality holds in (3.1) for some $y_0\in[-1,1]$. In particular, we deduce that Equation (3.1) is necessary for the existence of an arbitrary $\mathfrak{h}$-sphere, not necessarily rotational, since on the contrary the coexistence of an $\mathfrak{h}$-sphere and an entire $\mathfrak{h}$-graph would yield to a contradiction with the maximum principle.

Proposition 3.1 *Let $\mathfrak{h}$ be a C^1 function on $[-1,1]$, and suppose that there exists $y_*\in[0,1]$ (resp. $y_*\in[-1,0]$) such that $2\varepsilon\mathfrak{h}(y_*)=\sqrt{1-y_*^2}$. Then, there exists an upwards-oriented (resp. downwards-oriented) entire rotational $\mathfrak{h}$-graph Σ in $\mathbb{H}^2\times\mathbb{R}$. Moreover:*

1. *either Σ is a horizontal plane,*
2. *or Σ is a strictly convex graph.*

Proof: If $y_*=1$ (resp. $y_*=-1$), then $\mathfrak{h}(1)=0$ (resp. $\mathfrak{h}(-1)=0$), and we choose the surface Σ as the horizontal plane $\mathbb{H}^2\times\{t_0\}$, $t_0\in\mathbb{R}$, which is minimal. Then, by considering Σ with upwards orientation (resp. downwards orientation), its angle function is $\nu\equiv 1$ (resp. $\nu\equiv -1$), and so from (1.3) the result is trivial.

Now, suppose that $2\varepsilon\mathfrak{h}(y_*)=\sqrt{1-y_*^2}$ holds for some $y_*\in[0,1)$, assume $\mathfrak{h}(1)>0$ and define $y_0:=\max\{y\in[0,1):\ 2\mathfrak{h}(y)=\sqrt{1-y^2}\}$. Note that y_0 is well defined since $\mathfrak{h}(1)>0$, and by continuity $2\mathfrak{h}(y)>\sqrt{1-y^2}$ if $y\in(y_0,1]$. Hence, the horizontal graph $\Gamma_1=\Theta_1\cap\Gamma_1(y)$ defined by (2.5) has one connected component when we restrict $\Gamma_1(y)$ to $(y_0,1]$. Moreover, it satisfies $\Gamma_1(1)=0$ and $\Gamma_1(y)\to\infty$ as $y\to y_0$.

Let us take $\Lambda:=\{(x,y)\in\Theta_1 : y>y_0\}$, and define $\Lambda_+:=\{(x,y)\in\Lambda : x>\Gamma_1(y)\}$ and $\Lambda_-:=\{(x,y)\in\Lambda : x<\Gamma_1(y)\}$. Note that $\Lambda\setminus\Gamma_1$ is divided into two connected components Λ_+ and Λ_-, which are precisely monotonicity regions of Θ_1 because of item 4 in Lemma 2.1. Indeed, by Lemma 2.2 each orbit $y=y(x)$ in Λ_+ (resp. Λ_-) satisfies that $y'(x)<0$ (resp. $y'(x)>0$).

Now, from Corollary 2.5 it is known that there exists a unique orbit γ_+ in Θ_1 with $(0,1)$ as an endpoint. Additionaly, by the aforementioned monotonicity properties and Lemma 2.2 it is clear that γ_+ is globally contained in Λ_+. Thus, γ_+ can be globally defined by a graph $y=f(x)$, where $f\in C^1([0,\infty))$ satisfies $f(0)=1$, $f(x)\to y_1\geq y_0$ as $x\to\infty$, and $f'(x)<0$ for all $x>0$. As a matter of fact, Proposition 2.3 ensures us that $y_1=y_0$ (see Figure 1, left).

Consequently, the $\mathfrak{h}$-surface Σ_+ generated by the orbit γ_+ is an entire rotational graph in $\mathbb{H}^2\times\mathbb{R}$. It remains to prove that Σ_+ is strictly convex. On the one hand, since γ_+ is totally contained in Θ_1, hence $\varepsilon=1$, we deduce by (2.6) that κ_2 of Σ_+ is everywhere positive. On the other hand, γ_+ is totally contained in Λ_+, so (2.6) implies that κ_1 of Σ_+ is also everywhere positive concluding the proof of this case.

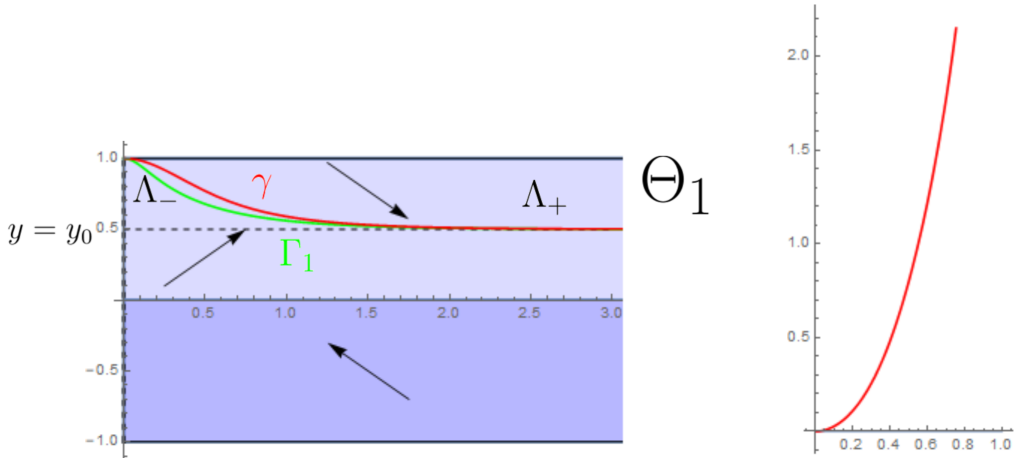

Figure 1: Left: the phase plane Θ_1, the regions Λ_+ and Λ_-, the curve Γ_1 in green and the orbit γ_+ in red. Right: the profile curve of an $\mathfrak{h}$-bowl in $\mathbb{H}^2 \times \mathbb{R}$. The prescribed function is $\mathfrak{h}(y) = \sqrt{3}(y - 0.25)$.

To finish, note that the case $\mathfrak{h}(-1) > 0$, $y_* \leq 0$ is treated analogously; and the two remaining cases, $\mathfrak{h}(1) < 0$, $y_* \geq 0$ and $\mathfrak{h}(-1) < 0$, $y_* \leq 0$, can be reduced to the previous ones by changing the orientation. □

These $\mathfrak{h}$-surfaces will be called $\mathfrak{h}$-*bowls*, in analogy with the theory of self-translating solitons of the mean curvature flow (see [Bue1, Bue2, LiMa]) that we extend with the previous result. See Figure 1, right, for a graphic of the profile curve of an $\mathfrak{h}$-bowl in $\mathbb{H}^2 \times \mathbb{R}$.

Secondly, we study the existence of *catenoid-type* rotational $\mathfrak{h}$-surfaces under appropiate conditions for the prescribed function $\mathfrak{h}$.

Proposition 3.2 *Let $\mathfrak{h}$ be a C^1 function on $[-1, 1]$, and suppose that $\mathfrak{h} \leq 0$ and $\mathfrak{h}(\pm 1) = 0$. Then, there exists a one-parameter family of properly embedded, rotational $\mathfrak{h}$-surfaces in $\mathbb{H}^2 \times \mathbb{R}$ of strictly negative extrinsic curvature at every point, and diffeomorphic to $\mathbb{S}^1 \times \mathbb{R}$. Each example is a bi-graph over $\mathbb{H}^2 - \mathbb{D}_{\mathbb{H}^2}(x_0)$, where $\mathbb{D}_{\mathbb{H}^2}(x_0) = \{x \in \mathbb{H}^2 : d_{\mathbb{H}^2}(x, (0,0)) < x_0\}$, for some $x_0 > 0$.*

Proof: Let $\Sigma(x_0)$ be the rotational $\mathfrak{h}$-surface generated by the arc-length parametrized curve $\alpha(s) = (x(s), z(s))$ with the following initial conditions

$$x(0) = x_0, \ z(0) = 0, \text{ and } z'(0) = 1, \text{ with } x_0 > 0.$$

Then, the orbit $\gamma(s) = (x(s), y(s))$ of system (2.4) associated to $\alpha(s)$ passes through the point $(x_0, 0)$ at $s = 0$. Moreover, γ is contained in Θ_1 around such a point, that is, $\varepsilon = 1$.

Observe that the curve Γ_1 given by (2.5) does not exist because of the assumption $\mathfrak{h} \leq 0$. Consequently, by item 4 in Lemma 2.1 there are two monotonicity regions of Θ_1 given by $\Lambda_+ := \{(x, y) \in \Theta_1 : y > 0\}$ and $\Lambda_- := \{(x, y) \in \Theta_1 : y < 0\}$. Then, from (2.4) we know that γ satisfies $x' > 0$ and $y' > 0$ in Λ_+, and $x' < 0$ and $y' > 0$ in Λ_-; see Figure 2, left.

Let us prove now that γ must be a proper arc strictly contained in Θ_1 satisfying $\gamma(s) \to (\infty, \pm 1)$ as $s \to \pm\infty$. First note that, the assumption $\mathfrak{h} \leq 0$ implies that given $y_0 \in (-1, 1)$, the equation

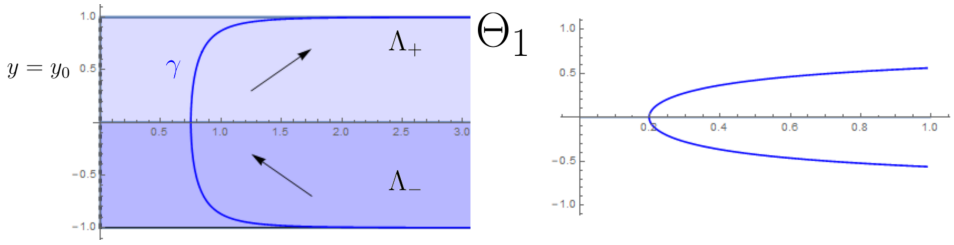

Figure 2: Left: the phase plane Θ_1, the monotonicity regions Λ_+ and Λ_-, and an orbit γ in blue. Right: the profile curve of an $\mathfrak{h}$-catenoid in $\mathbb{H}^2 \times \mathbb{R}$. The prescribed function is $\mathfrak{h}(y) = y^2 - 1$.

$2\mathfrak{h}(y_0) = \sqrt{1 - y_0^2}$ has no solutions, so from Proposition 2.3 γ cannot satisfy $\gamma(s) \to (\infty, y_0)$ as $s \to \pm\infty$. Second, since $\mathfrak{h} \in C^1$ and $\mathfrak{h}(\pm 1) = 0$, from the uniqueness of the Cauchy problem associated to (2.4), the curve $(s, \pm 1)$, $s > 0$, is a solution to (2.4) which corresponds to a horizontal plane $\mathbb{H}^2 \times \{t_0\}$, $t_0 \in \mathbb{R}$, endowed with $\pm\partial_z$ as unit normal, that is, $\gamma(s)$ cannot satisfy $\gamma(s_0) = (x_0, \pm 1)$ for some $s_0 \in \mathbb{R}$. Finally, it remains to show that $\gamma(s)$ cannot converge to some $(x_0, \pm 1)$, $x_0 > 0$, as $s \to \pm\infty$. Otherwise, there would exist $s_0 \in \mathbb{R}$ such that for $|s| > |s_0|$, $x(s)$ is a monotonous function satisfying $x(s) \to x_0$ as $|s| \to \infty$. Thus, the mean value theorem ensures us that $x'(s) = y(s) \to 0$, which is a contradiction with the fact that $y(s) \to \pm 1$.

Thus, $\Sigma(x_0)$ is a bi-graph in $\mathbb{H}^2 \times \mathbb{R}$ over $\Omega(x_0) := \mathbb{H}^2 - \mathbb{D}_{\mathbb{H}^2}(x_0)$, with the topology of $\mathbb{S}^1 \times \mathbb{R}$. Indeed, $\Sigma(x_0) = \Sigma_1 \cup \Sigma_2$ where both Σ_i are graphs over $\Omega(x_0)$ with $\partial\Sigma_i = \partial\Omega(x_0)$ and Σ_i meets the horizontal plane $\mathbb{H}^2 \times \{0\}$ in an orthogonal way along $\partial\Sigma_i$ (see Figure 2, right, for a plot of the profile curve).

It remains to prove that the extrinsic curvature of $\Sigma(x_0)$ is strictly negative. By (2.4) we get $y'(s) > 0$ for all s, so from (2.6) we derive $\kappa_1 < 0$ and $\kappa_2 > 0$ at every $p \in \Sigma$. □

This one-parameter family of rotational $\mathfrak{h}$-surfaces is a generalization of the usual minimal catenoids in $\mathbb{H}^2 \times \mathbb{R}$, and this is the reason for calling them $\mathfrak{h}$-*catenoids*. As happens for the minimal catenoids, the $\mathfrak{h}$-catenoids are parametrized by their *necksizes*, i.e. the distance of their *waists* to the axis of rotation.

4 Classification of rotational $\mathfrak{h}$-surfaces with linear prescribed mean curvature

Our aim in this section is to classify the rotational examples of the following class of $\mathfrak{h}$-surfaces:

Definition 4.1 *An oriented surface Σ immersed in $\mathbb{H}^2 \times \mathbb{R}$ is an $\mathfrak{h}_\lambda$-surface if its mean curvature function H_Σ satisfies*

$$H_\Sigma(p) = \mathfrak{h}_\lambda(\nu(p)) = a\nu(p) + \lambda, \ \forall p \in \Sigma, \qquad a, \lambda \in \mathbb{R}. \tag{4.1}$$

Note that if $a = 0$, then we are studying surfaces with constant mean curvature equal to λ. Also, if $\lambda = 0$ the $\mathfrak{h}_\lambda$-surfaces are translating solitons of the mean curvature flow, see [Bue1, Bue2, LiMa]. Hence, we suppose that a, λ are not null in order to avoid these cases. After a conformal change of the

metric in $\mathbb{H}^2$ and a dilation in the factor $\mathbb{R}$ (see the proof of Theorem 2.1 in [AEG]), we can suppose $a = 1$ in Equation (4.1). Moreover, if Σ is an $\mathfrak{h}_\lambda$-surface, then Σ with its opposite orientation is an $\mathfrak{h}_{-\lambda}$-surface. Therefore, we will assume $\lambda > 0$ without losing generality. In particular this implies that $\varepsilon\mathfrak{h}(0) > 0$ if and only if $\varepsilon = 1$, and consequently the equilibrium $e_0 = (\operatorname{arctanh}(\frac{1}{2\varepsilon\mathfrak{h}(0)}), 0)$ can only exist in Θ_1. The CMC vertical cylinder generated by e_0 will be denoted by C_λ.

First, we announce two technical results that will be useful in the sequel. The first one was originally proved by López in [Lop] for surfaces in $\mathbb{R}^3$ whose mean curvature is given by Equation (4.1).

Lemma 4.2 *There do not exist closed $\mathfrak{h}_\lambda$-surfaces in $\mathbb{H}^2 \times \mathbb{R}$.*

Proof: Arguing by contradiction, suppose that Σ is a closed $\mathfrak{h}_\lambda$-surface in $\mathbb{H}^2 \times \mathbb{R}$. If $h : \Sigma \to \mathbb{R}$ denotes the *height function* of Σ, it is known that the Laplace-Beltrami operator Δ_Σ of h is $\Delta_\Sigma h = 2H_\Sigma\langle \eta, \partial_z\rangle$. Since Σ is an $\mathfrak{h}_\lambda$-surface, we get

$$\Delta_\Sigma h = 2\langle \eta, \partial_z\rangle^2 + 2\lambda\langle \eta, \partial_z\rangle.$$

We integrate this equation in Σ. By the divergence theorem and since $\partial\Sigma = \varnothing$, we have

$$0 = \int_\Sigma \langle \eta, \partial_z\rangle^2 d\Sigma + \lambda \int_\Sigma \langle \eta, \partial_z\rangle d\Sigma.$$

The second integral is zero by the divergence theorem, since the constant vector field ∂_z has zero divergence. So, the first integral vanishes, that is, Σ is contained in a cylindrical surface of the form $\beta \times \mathbb{R}$, $\beta \subset \mathbb{H}^2$ being a curve, which contradicts that Σ is compact. □

The second result forbids the existence of closed orbits in the phase plane of system (2.4) for some prescribed functions $\mathfrak{h}$. It follows from Bendixson-Dulac theorem, a classical result which appears in most textbooks on differential equations; see e.g. [ADL].

Theorem 4.3 *Let $\mathfrak{h}$ be a C^1 function on $[-1, 1]$ such that $\mathfrak{h}'(y) \neq 0$, $\forall y \in (-1, 1)$. Then, there do not exist closed orbits in Θ_ε.*

Proof: Let us write system (2.4) as

$$\begin{pmatrix} x \\ y \end{pmatrix}' = \begin{pmatrix} y \\ \dfrac{1-y^2}{\tanh x} - 2\varepsilon\mathfrak{h}(y)\sqrt{1-y^2} \end{pmatrix} = \begin{pmatrix} P(x,y) \\ Q(x,y) \end{pmatrix},$$

and define the function $\alpha : \Theta_\varepsilon \to \mathbb{R}$ and the vector field $V : \Theta_\varepsilon \to \Theta_\varepsilon$ as

$$\alpha(x,y) = \frac{\sinh x}{\sqrt{1-y^2}}, \qquad V(x,y) = \alpha(x,y)(P(x,y), Q(x,y)).$$

Arguing by contradiction, suppose that there exists some closed orbit $\overline{\gamma}$ in Θ_ε and name Ω to its inner region. A simple computation yields $\operatorname{div} V = (\alpha P)_x + (\alpha Q)_y = -2\varepsilon\mathfrak{h}'(y)\sinh x$, which has constant sign since $x > 0$ in Θ_ε and $\mathfrak{h}'(y) \neq 0$. Therefore, the divergence theorem in Ω yields

$$0 \neq \int_\Omega \operatorname{div} V = \int_\gamma \langle V, \mathbf{n}_\gamma\rangle = 0,$$

where $\mathbf{n}_\gamma$ is the unit normal to the curve γ. Recall that the last integral vanishes since V is everywhere tangent to γ. This contradiction proves the result. □

In particular, the prescribed function $\mathfrak{h}_\lambda(y) = y + \lambda,\ \lambda > 0$ lies in the hypothesis of Theorem 4.3, hence the phase plane Θ_ε of system (2.4) for $\mathfrak{h}_\lambda$-surfaces does not have closed orbits.

Now, suppose that Σ is a rotational $\mathfrak{h}_\lambda$-surface generated by an arc-length parametrized curve $\alpha(s) = (x(s), z(s))$. Then, (1.3) and (2.2) yields

$$2H_\Sigma = 2(x' + \lambda) = x'z'' - x''z' + \frac{z'}{\tanh x}. \tag{4.2}$$

Our first goal is to study the structure of the orbits around $e_0 = (\operatorname{arctanh}(\frac{1}{2\lambda}), 0)$. Recall that e_0 exists if and only if $\lambda > 1/2$; otherwise, arctanh is not well defined. The *linearized* system of (2.4) at e_0 is given by

$$\begin{pmatrix} 0 & 1 \\ 1 - 4\lambda^2 & -2 \end{pmatrix}, \tag{4.3}$$

whose eigenvalues are

$$\mu_1 = -1 + \sqrt{2 - 4\lambda^2}, \qquad \text{and} \qquad \mu_2 = -1 - \sqrt{2 - 4\lambda^2}.$$

From standard theory of non-linear autonomous systems we derive:

Lemma 4.4 *In the above conditions, we have:*

- *If $\lambda > \dfrac{\sqrt{2}}{2}$, then μ_1 and μ_2 are complex conjugate with negative real part. Thus, e_0 has an* inward spiral *structure, and every orbit close enough to e_0 converges asymptotically to it spiraling around infinitely many times.*

- *If $\lambda = \dfrac{\sqrt{2}}{2}$, then $\mu_1 = \mu_2 = -1$. Thus, e_0 is an asymptotically stable improper node, and every orbit close enough to e_0 converges asymptotically to it, maybe spiraling around a finite number of times.*

- *If $0 < \lambda < \dfrac{\sqrt{2}}{2}$, then μ_1 and μ_2 are different and real. Thus, e_0 is an asymptotically stable node and has a* sink *structure, hence every orbit close enough to e_0 converges asymptotically to it* directly*, i.e. without spiraling around.*

Now we stand in position to prove Theorem 1.2.

Proof of Theorem 1.2: Note that the behavior of the orbits in each phase plane Θ_ε depends on the curve Γ_ε and the monotonicity regions generated by it. Consequently, we analyze three different cases for λ: $\lambda > \sqrt{5}/2$, $\lambda = \sqrt{5}/2$ and $0 < \lambda < \sqrt{5}/2$.

Case $\lambda > \sqrt{5}/2$

Let us assume $\lambda > \sqrt{5}/2$. For $\varepsilon = 1$, the curve Γ_1 given by (2.5) is a compact connected arc in Θ_1 joining $(0,1)$ and $(0,-1)$, whereas for $\varepsilon = -1$, since $\mathfrak{h}$ is positive, the curve Γ_{-1} does not exist in Θ_{-1}. As a matter of fact, by item 4 in Lemma 2.1 we know that there are four monotonicity regions in Θ_1 which will be denoted by $\Lambda_1, \ldots, \Lambda_4$, and there are only two monotonicity regions in Θ_{-1} which will be denoted by Λ_+ and Λ_-. See Figure 3.

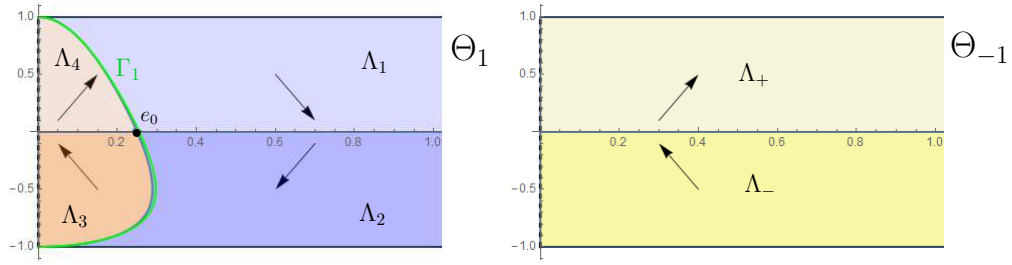

Figure 3: The phase planes Θ_1 and Θ_{-1} for $\lambda > \sqrt{5}/2$ with their monotonicity regions and the direction of the motion of the orbits at each of them.

Now, by using Corollary 2.5 it is clear that there exists a unique orbit γ_+ (resp. γ_-) in Θ_1 with $(0,1)$ (resp. $(0,-1)$) as an endpoint.

On the one hand, let us study the behavior of γ_+. Firstly, we can suppose that such an orbit satisfies $\gamma_+(0) = (0,1)$ in Θ_1, i.e., it generates an arc-length parametrized curve $\alpha_+(s)$ intersecting orthogonally the rotation axis with upwards oriented unit normal at $s = 0$. Because of the monotonicity properties, $\gamma_+(s)$ is strictly contained in the region Λ_1 for $s > 0$ small enough. However, the orbit γ_+ cannot stay forever in Λ_1, otherwise γ_+ would be globally defined by a graph $y = f(x)$ such that

$$f(0) = 1, \quad f'(x) < 0 \ \ \forall x > 0 \quad \text{and} \quad \lim_{x\to\infty} f(x) = c \in [0,1).$$

This contradicts Proposition 2.3 since $\lambda > \sqrt{5}/2$ and hence $2\mathfrak{h}_\lambda(y) = 2(y+\lambda) > \sqrt{1-y^2}$. Thus, $\gamma_+(s)$ intersects the axis $y = 0$ in an orthogonal way at a point $(x_+, 0)$ with $x_+ > \operatorname{arctanh}\left(\frac{1}{2\lambda}\right)$ at some finite instant $s_+ > 0$.

On the other hand, for the orbit γ_- we assume that $\gamma_-(0) = (0,-1)$ in Θ_1, that is, it generates an arc-length parametrized curve $\alpha_-(s)$ intersecting orthogonally the axis of rotation with downwards oriented unit normal at $s = 0$. By an analogous reasoning, we can assert that $\gamma_-(s)$ intersects $y = 0$ orthogonally at $(x_-, 0)$ with $x_- > \operatorname{arctanh}\left(\frac{1}{2\lambda}\right)$ at some finite instant $s_- < 0$.

Now, we prove that $x_+ < x_-$ arguing by contradiction. First, see that if $x_+ = x_- = \bar{x}$, by uniqueness of the Cauchy problem the orbits γ_+ and γ_- could be smoothly glued together constructing a larger orbit $\bar{\gamma}$ which would be a compact arc joining the points $(0,1)$, $(\bar{x},0)$ and $(0,-1)$ and so the rotational $\mathfrak{h}_\lambda$-surface generated would be a rotational $\mathfrak{h}$-sphere, which is impossible because of Lemma 4.2. Additionally, if $x_+ > x_-$, it would mean that γ_- intersect the axis $y = 0$ at the left-hand side of γ_+, and consequently the only possibility for γ_- would be to enter the region Λ_1, later Λ_4 and after that Λ_3. In any case, γ_- cannot converge to any point $(0,y)$, $|y| < 1$ in virtue of Lemma 2.4. Repeating this process, and since γ_- cannot self-intersect nor converge to a closed orbit by Theorem 4.3, γ_- finishes converging asymptotically to the equilibrium e_0 as $s \to -\infty$, spiriling around infinitely many times. This is a contradiction with the inward spiral structure of

e_0, since this orbit would tend to escape from e_0 when s increases. See Figure 4.

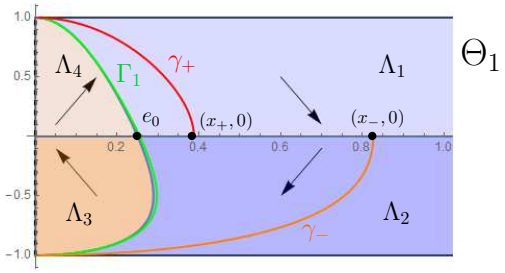

Figure 4: The phase plane Θ_1 for $\lambda > \sqrt{5/2}$ with the configurarion of the orbits γ_+ and γ_-, plotted in red and orange, respectively, until they intersect the axis $y = 0$.

Let us continue by analyzing the global behavior of both orbits. Firstly, when γ_+ passes through $(x_+, 0)$, it enters to Λ_2 but cannot intersect γ_-, so γ_+ has to enter to Λ_3. After that, due to the monotonicity properties and Lemma 2.4 we deduce that γ_+ has to enter to Λ_4 and intersect Γ_1. Since γ_+ cannot self-intersect nor converge to a limit closed orbit in Θ_1 in virtue of Theorem 4.3, the only possibility for γ_+ is to repeat this behavior and eventually converge asymptotically to the equilibrium e_0 (see the plot of γ_+ in Figure 5 top-left). Furthermore, since $\lambda > \sqrt{2}/2$, γ_+ spirals around e_0 infinitely many times.

In this way, γ_+ generates the curve $\alpha_+(s) = (x_+(s), z_+(s))$ satisfying: the $x_+(s)-$coordinate is bounded by the value x_+ and converges to $\operatorname{arctanh}\left(\frac{1}{2\lambda}\right)$; and the $z_+(s)$-coordinate is strictly increasing since $\gamma_+ \subset \Theta_1$, hence $z_+'(s) > 0$. Then, $\alpha_+(s)$ is an embedded curve that converges to the line $x = \operatorname{arctanh}\left(\frac{1}{2\lambda}\right)$ intersecting it infinitely many times. Therefore, after rotating such a curve around the rotation axis, we derive that the generated surface Σ_+ is a properly embedded, simply connected $\mathfrak{h}_\lambda$-surface that converges to the CMC cylinder C_λ intersecting it infinitely many times. See Σ_+ in Figure 5 top-right.

Now we focus on γ_-, which intersects the axis $y = 0$ at the point $\gamma_-(s_-) = (x_-, 0)$ at some finite instant $s_- < 0$. So, when the parameter $s < s_-$ decreases, γ_- enters to Λ_1. Bearing in mind that γ_+ and γ_- cannot intersect, from the monotonicity properties we deduce that γ_- has as endpoint $\gamma_-(s_1) = (x_1, 1)$ with $0 < x_1 < x_-$ and $s_1 < s_-$. Then, γ_- generates the curve $\alpha_-(s) = (x_-(s), z_-(s))$ satisfying that: $x_-(s_1) = x_1$ and $x_-'(s_1) = 1$, so from (4.2) we get $z_-''(s_1) > 0$, i.e., the height of α_- reaches a minimum at s_1. If we name Σ_- to the $\mathfrak{h}_\lambda$-surface associated to γ_- and generated by rotating $\alpha_-(s)$, the image of the points $\alpha_-(s_1)$ under such rotation corresponds to points on the boundary of Σ_- having unit normal ∂_z.

Therefore, for $s < s_1$, s close enough to s_1, the height function $z_-(s)$ of $\alpha_-(s)$ is decreasing, i.e. $z_-'(s) < 0$. Consequently, $\alpha_-(s)$ for $s < s_1$ close enough to s_1 generates an orbit in Θ_{-1} (since $\varepsilon = \operatorname{sign}(z_-') = -1$), which will be named γ_- for saving notation. Hence, the orbit $\gamma_-(s)$ *continues* from Θ_1 to Θ_{-1} as s decreases from $s = s_1$. At this point, the continuation of γ_- between the phase planes $\Theta_{\pm 1}$ has to be understood as the extension of Σ_- by solving the Cauchy problem for rotational vertical $\mathfrak{h}_\lambda$-graphs having the same vertical unit normal.

Hence, $\gamma_-(s)$ belongs to Θ_{-1} for $s < s_1$ close enough to s_1 and lies in the region Λ_+. Once again, by monotonicity, γ_- must intersect the axis $y = 0$ orthogonally and enter to Λ_-. As γ_-

cannot stay forever in Λ_- with $x_-(s) \to \infty$ for $s \to -\infty$, we derive that there exists $s_2 < s_1$ such that $\gamma_-(s_2) = (x_2, -1)$ (see the plot of γ_- in Figure 5 left). Repeating this process indefinitely, we construct a complete, arc-length parametrized curve $\alpha_-(s)$ with infinitely many self-intersections, whose height function increases and decreases until reaching the rotation axis. Hence, the generated rotational $\mathfrak{h}_\lambda$-surface Σ_- is properly immersed (with self-intersections) and simply connected. See Figure 5, bottom right.

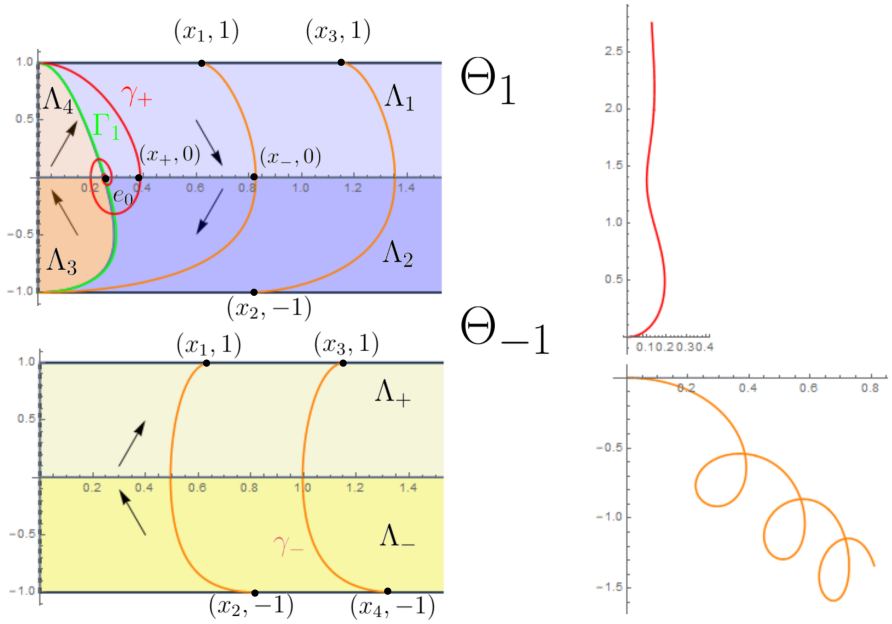

Figure 5: Left: the phase planes Θ_1 and Θ_{-1} for $\lambda > \sqrt{5}/2$ and the orbits γ_+ and γ_-, plotted in red and orange, respectively. Right: the profile curve of the corresponding rotational $\mathfrak{h}_\lambda$-surfaces Σ_+ and Σ_-.

Case $\lambda = \sqrt{5}/2$

Assume that $\lambda = \sqrt{5}/2$. For $\varepsilon = 1$, Γ_1 is formed by two connected arcs $\Gamma_1^{\pm}$, each of them having the point $(0, \pm 1)$ as endpoint respectively, and both having the line $y = -2/\sqrt{5}$ as an asymptote. From item 4 in Lemma 2.1 we find five monotonicity regions in the phase plane Θ_1 denoted by $\Lambda_1, \ldots, \Lambda_5$ (see Figure 6 left). For $\varepsilon = -1$, the phase plane Θ_{-1} is exactly the same that in the previous case $\lambda > \sqrt{5}/2$.

From Corollary 2.5 we can assert that there exists a unique orbit γ_+ (resp. γ_-) in Θ_1 with $(0, 1)$ (resp. $(0, -1)$) as an endpoint.

Regarding the orbit γ_+, it converges to $e_0 = (\operatorname{arctanh}\frac{1}{\sqrt{5}}, 0)$ as $s \to \infty$ spiraling around it infinitely many times in the same fashion as the orbit γ_+ studied in the previous case $\lambda > \sqrt{5}/2$, see Figure 6 left. Consequently, its corresponding $\mathfrak{h}_\lambda$-surface Σ_+ has the same behavior as the one shown in Figure 5, top right.

Now, consider the orbit γ_- such that $\gamma_-(0) = (0, -1)$. It is clear that $\gamma_-(s)$ is totally contained in Λ_3 and when the parameter s tends to $-\infty$, the orbit $\gamma_-(s)$ converges to the line $y = -2/\sqrt{5}$.

Note that $\gamma_-(s)$ cannot converge to other line $y = y_0$, $y_0 \in (-1, -2/\sqrt{5})$ in virtue of Proposition 2.3 (see the plot of γ_- in Figure 6 left). Therefore, the generated $\mathfrak{h}_\lambda$-surface Σ_- is an entire, strictly convex graph whose angle function tends to the value $-2/\sqrt{5}$. See Figure 6 right.

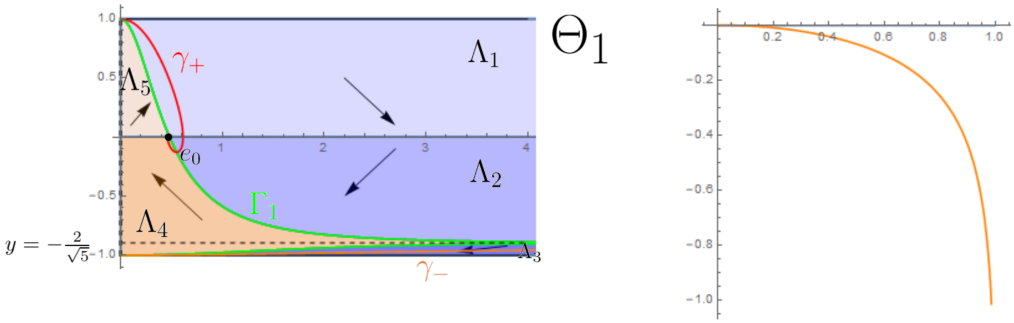

Figure 6: Left: the phase plane Θ_1 for $\lambda = \sqrt{5}/2$ and the orbits γ_+ and γ_-, plotted in red and orange, respectively. Right: the profile curve of the corresponding rotational $\mathfrak{h}_\lambda$-surface Σ_-.

Case $\lambda < \sqrt{5}/2$

We begin by analyzing the behavior of Γ_ε in Θ_ε. Recall that the equilibrium e_0 exists in Θ_1 if and only if $\lambda > 1/2$. Additionally, we define the candidates of asymptotes for Γ_ϵ as:

$$y_0^+ := \frac{1}{5}(-4\lambda + \sqrt{5 - 4\lambda^2}), \quad \text{and} \quad y_0^- := \frac{1}{5}(-4\lambda - \sqrt{5 - 4\lambda^2}).$$

Let us distinguish further cases of λ:

1. If $\lambda > 1$, then Γ_1 is a disconnected arc having two connected components Γ_1^+ and Γ_1^-, with Γ_+ (resp. Γ_-) having the point $(0, 1)$ (resp. $(0, -1)$) as an endpoint and the line $y = y_0^+$ (resp. $y = y_0^-$) as asymptote; see Figure 7. The curve Γ_{-1} does not exist in Θ_{-1} as in the previous cases.

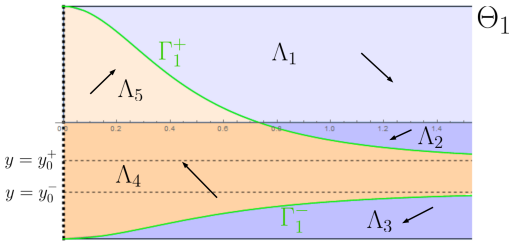

Figure 7: The phase plane Θ_1 for some $\lambda \in (1, \sqrt{5}/2)$.

2. If $\lambda = 1$, then Γ_1 is a connected arc having $(0, 1)$ as endpoint and the line $y = y_0^+ = -3/5$ as asymptote. The line $y = y_0^- = -1$ does not appear. The curve Γ_{-1} does not exist in Θ_{-1}.

3. If $\lambda < 1$, then Γ_1 is a connected arc having $(0, 1)$ as endpoint and the line $y = y_0^+$ as asymptote. Moreover, $y_0^+ \geq 0$ if and only if $\lambda \leq 1/2$. The curve Γ_{-1} is a connected arc having $(0, -1)$ as endpoint and the line $y = y_0^-$ as an asymptote; see Figure 8.

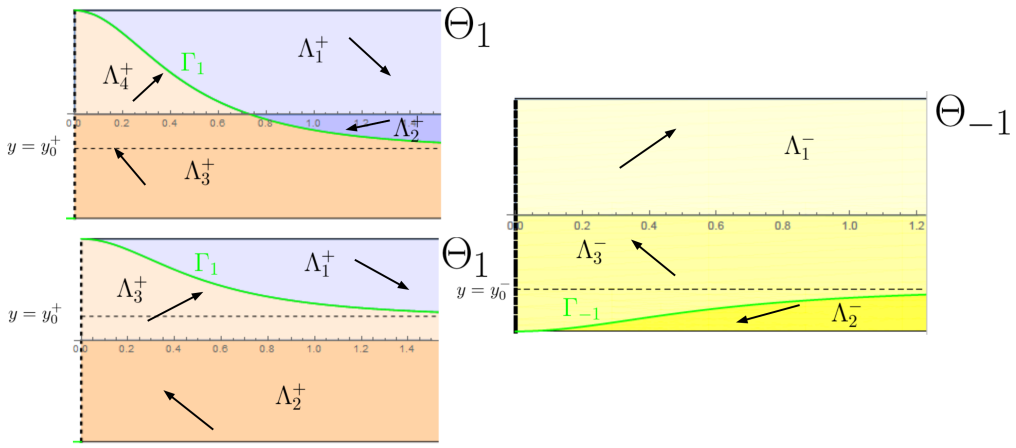

Figure 8: Top left: the phase plane Θ_1 for $\lambda > 1/2$. Bottom left: the phase plane Θ_1 for $\lambda \leq 1/2$. Right: the phase plane Θ_{-1} for $\lambda < 1$.

Now, we study the behavior of the orbits. Once again, the existence of the orbit $\gamma_+(s)$ in Θ_1 such that $\gamma(0) = (0, 1)$ follows from Corollary 2.5. Then, if we suppose that $\lambda \leq 1/2$, $\gamma_+(s)$ stays in Λ_1^+ as it converges to the line $y = y_0^+$, and so Σ_+ is an entire, strictly convex graph. Otherwise, i.e., if $\lambda > 1/2$, the equilibrium e_0 exists. Since no closed orbit exists in virtue of Theorem 4.3, γ_+ converges to e_0 as $s \to \infty$, and its behavior is detailed in Lemma 4.4. Consequently, Σ_+ is a properly embedded, simply connected $\mathfrak{h}_\lambda$-surface and:

- If $\lambda > \dfrac{\sqrt{2}}{2}$, Σ_+ intersects C_λ infinitely many times.
- If $\lambda = \dfrac{\sqrt{2}}{2}$, Σ_+ intersects C_λ a finite number of times.
- If $\lambda < \dfrac{\sqrt{2}}{2}$, Σ_+ is a strictly convex graph contained in the solid cylinder bounded by C_λ and converging asymptotically to it.

For the study of the orbit $\gamma_-(s)$ such that $\gamma_-(0) = (0, -1)$ we have to distinguish between the cases $\lambda > 1$, $\lambda = 1$, $\lambda < 1$. This discussion will deeply influence the outcome of Corollary 2.5:

1. If $\lambda > 1$, then $\mathfrak{h}_\lambda(-1) > 0$ and $\gamma_-(s)$ lies in Θ_1.
2. If $\lambda = 1$, then $\mathfrak{h}_\lambda(-1) = 0$ and $\gamma_-(s)$ does not exist in either Θ_1 or Θ_{-1}.
3. If $\lambda < 1$, then $\mathfrak{h}_\lambda(-1) < 0$ and $\gamma_-(s)$ lies in Θ_{-1}.

If $\lambda = 1$, horizontal minimal planes downwards oriented are $\mathfrak{h}_1$-surfaces. Consequently, the uniqueness of the Cauchy problem of (2.4) extends to the line $y = -1$ and so no orbit can have and endpoint at this line.

If $\lambda \neq 1$, by monotonicity and Proposition 2.3, the only possibility for $\gamma_-(s)$ is to converge to the line $y = y_0^-$, and so Σ_- is a downwards oriented, strictly convex, entire graph. For $\lambda > 1$, the height of Σ_- tends to minus infinity; for $\lambda < 1$, the height of Σ_- tends to infinity.

This concludes the classification of the rotational $\mathfrak{h}_\lambda$-surfaces that intersect the axis of rotation. □

To finish, we prove Theorem 1.3.

Proof of Theorem 1.3: First, the equilibrium $e_0 = (\operatorname{arctanh}\frac{1}{2\lambda}, 0)$ exists if and only if $\lambda > \frac{1}{2}$. This equilibrium generates the cylinder C_λ with CMC equal to λ and vertical rulings. For the remaining $\mathfrak{h}_\lambda$-surfaces, we distinguish again three cases depending on λ. Take into account that the structure of the phase planes Θ_1 and Θ_{-1} has been just studied in the previous proof. See Figure 3 for $\lambda > \sqrt{5}/2$, Figure 6 for $\lambda = \sqrt{5}/2$ and Figures 7 and 8 for $\lambda < \sqrt{5}/2$.

Case $\lambda > \sqrt{5}/2$

Let us take $x_0 > \operatorname{arctanh}(\frac{1}{2\lambda})$ and let $\gamma(s)$ be the orbit in Θ_1 passing through the point $(x_0, 0)$ at the instant $s = 0$. For $s < 0$, γ has as endpoint some $(x_1, 1)$, $x_1 > 0$ (if $x_1 = 0$, $\gamma = \gamma_+$), and for $s > 0$ either converges to e_0 as $s \to \infty$ or has another endpoint of the form $(x_2, -1)$, $x_2 > 0$ (again, if $x_2 = 0$, $\gamma = \gamma_-$). In the second case, the orbit γ continues in Θ_{-1} as a compact arc and then goes again in Θ_1; see Figure 9, left. After a finite number of iterations, the orbit γ eventually converges to e_0 spiraling around it infinitely many times.

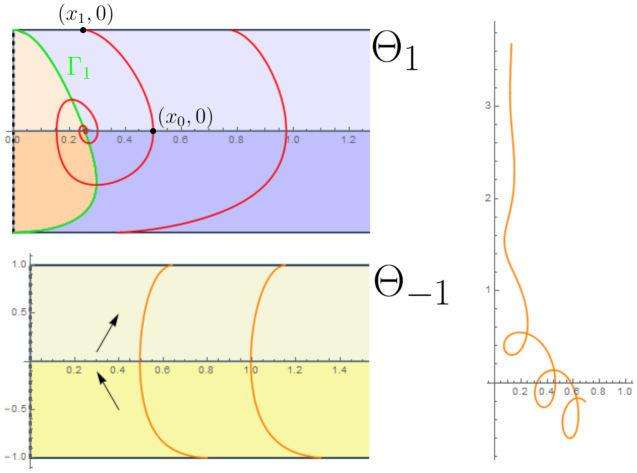

Figure 9: Left: the phase planes Θ_1 and Θ_{-1} for $\lambda > \sqrt{5}/2$ and an orbit γ. Right: the profile curve of a rotational $\mathfrak{h}_\lambda$-surface corresponding to an orbit γ.

This configuration ensures us that the $\mathfrak{h}_\lambda$-surface generated by γ is properly immersed, non-embedded, and diffeomorphic to $\mathbb{S}^1 \times \mathbb{R}$. One end converges to C_λ intersecting it infinitely many times, and the other end has unbounded distance to the axis of rotation, looping and self-intersecting infinitely many times (see Figure 9, right).

Case $\lambda = \sqrt{5}/2$

Firstly, let us fix some $x_0 > \operatorname{arctanh}(\frac{1}{\sqrt{5}})$ and consider the orbit $\gamma_1(s)$ passing through $(x_0, 0)$ at $s = 0$. For $s < 0$, $\gamma_1(s)$ is contained in Λ_1, so it satisfies $\gamma_1(s_1) = (x_1, 1)$ as endpoint for some $s_1 < 0$. Hence, for $s < s_1$, $\gamma_1(s)$ lies in Θ_{-1} and is a compact arc whose other endpoint is located at some $\gamma_1(s_2) = (x_2, -1)$. Finally, for $s < s_2$, $\gamma_1(s)$ lies in the monotonicity region Λ_3 in Θ_1 and stays there as it converges to the line $y = -2/\sqrt{5}$ as $s \to -\infty$; see Figure 10, top left, the red orbit.

For $s > 0$, $\gamma_1(s)$ enters to Λ_2, then goes inside Λ_4 and intersects $y = 0$ for the second time in some $(\widehat{x}_0, 0)$ with $\widehat{x}_0 > 0$. It is clear that when x_0 increases, then $\widehat{x}_0$ decreases and so $\widehat{x}_0 \to x_\infty \geq 0$ as $x_0 \to \infty$. Also, note that $\gamma_1(s)$ stays always above the line $y = -2/\sqrt{5}$ since the minimum of its $y(s)$-coordinate is at the intersection of $\gamma_1(s)$ with Γ_1. In this setting, we claim that $x_\infty > 0$.

Arguing by contradiction, suppose that $x_\infty = 0$ and consider an orbit $\sigma(s)$ such that $\sigma(0)$ lies in Λ_4 and is located below the line $y = -2/\sqrt{5}$. Then, for $s > 0$ in virtue of Proposition 2.4 and by monotonicity, $\sigma(s)$ has to reach the axis $y = 0$ at a point $(\widehat{r}_1, 0)$ for some finite instant. Due to the definition of x_∞ and the assumption $x_\infty = 0$, there exists $r > e_0$ and an orbit γ such that $\gamma(0) = (r, 0)$ and $\gamma(s_1) = (\widehat{r}, 0)$ with $0 < \widehat{r} < \widehat{r}_1$, for some $s_1 > 0$. Hence, σ and γ intersect each other, which is a contradiction with the uniqueness of the Cauchy problem.

Secondly, let be $r_0 > 0$ and take $\gamma_2(s)$ the orbit such that $\gamma_2(0) = (r_0, -\sqrt{2}/5)$. For $s < 0$, $\gamma_2(s)$ lies in Λ_4, intersects the curve Γ_1^-, enters Λ_3 and converges to the line $y = -2/\sqrt{5}$. For $s > 0$, $\gamma_2(s)$ lies in Λ_4 until intersecting $y = 0$ at some $(\widetilde{r_0}, 0)$. Moreover, as r_0 increases $\widetilde{r_0}$ also increases, and so $\widetilde{r_0} \to r_\infty$ as $r_0 \to \infty$. In particular, $r_\infty \leq x_\infty$. For $s \to \infty$, $\gamma_2(s)$ converges asymptotically to e_0, spiraling around it infinitely many times; see Figure 10, top left, the blue orbit.

Finally, take some $\xi_0 \in [r_\infty, x_\infty]$ and let $\gamma_3(s)$ be the orbit such that $\gamma_3(0) = (\xi_0, 0)$. For $s > 0$ it is clear that $\gamma_3(s)$ converges asymptotically to e_0, spiraling around it infinitely many times. Because of how r_∞ and x_∞ have been defined, for $s < 0$ the orbit $\gamma_3(s)$ cannot intersect Γ_1^- nor intersect $y = -2/\sqrt{5}$. Thus, the only possibility for $\gamma_3(s)$ is to converge to the line $y = -2/\sqrt{5}$ with strictly decreasing $y(s)$-coordinate; see Figure 10, top left, the purple orbit.

Thus, each orbit γ_i, $i = 1, 2, 3$ generates a properly immersed $\mathfrak{h}_\lambda$-surface Σ_i, diffeomorphic to $\mathbb{S}^1 \times \mathbb{R}$, with one end converging asymptotically to the CMC cylinder C_λ and the other being a graph outside a compact set. Moreover, Σ_1 is non-embedded, while Σ_2 and Σ_3 have monotonous height and in particular are embedded; see Figure 10, right.

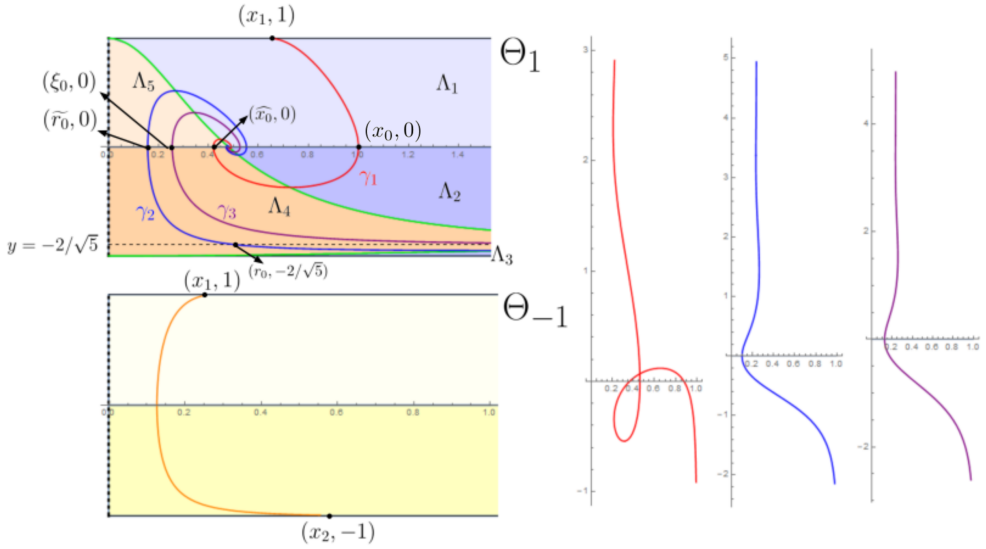

Figure 10: Left: the phase planes Θ_1 and Θ_{-1} for $\lambda = \sqrt{5}/2$ and the three types of orbits γ_1, γ_2 and γ_3. Right: the profile curve of the corresponding rotational $\mathfrak{h}_\lambda$-surfaces.

Case $\lambda < \sqrt{5}/2$

In this final case, we also distinguish between values of λ. Note that the equilibrium $e_0 = (\operatorname{arctanh}(\frac{1}{2\lambda}), 0)$ exists if and only if $\lambda > 1/2$. Again, we define

$$y_0^+ := \frac{1}{5}(-4\lambda + \sqrt{5 - 4\lambda^2}), \quad \text{and} \quad y_0^- := \frac{1}{5}(-4\lambda - \sqrt{5 - 4\lambda^2}).$$

1. Case $1 \leq \lambda < \sqrt{5}/2$. The structure of the phase plane Θ_1 (resp. Θ_{-1}) is the same as the one in Figure 7 (resp. Figure 3, right). Recall that $y_0^- = -1$ in Θ_1 for $\lambda = 1$ and there are only four monotonicity regions. The same reasoning as in the case $\lambda = \sqrt{5}/2$ ensures us that we can construct three types of orbits (see Figure 10) and also the points x_∞ and r_∞:

   - $\gamma_1(s)$ such that $\gamma_1(0) = (x_0, 0)$ with $x_0 > \operatorname{arctanh}(\frac{1}{2\lambda})$ and $\gamma_1(s) \to e_0$ as $s \to \infty$.
   - $\gamma_2(s)$ such that $\gamma_2(0) = (r_0, y_0^+)$ with $r_0 > 0$, $\gamma_2(s) \to e_0$ as $s \to \infty$ and $\gamma_2(s) \to y_0^-$ as $s \to -\infty$.
   - $\gamma_3(s)$ such that $\gamma_3(0) = (\xi_0, 0)$ with $\xi_0 \in [r_\infty, x_\infty]$, $\gamma_3(s) \to e_0$ as $s \to \infty$ and $\gamma_3(s) \to y_0^+$ as $s \to -\infty$.

   Again, each orbit γ_i, $i = 1, 2, 3$ generates a properly immersed $\mathfrak{h}_\lambda$-surface Σ_i that is diffeomorphic to $\mathbb{S}^1 \times \mathbb{R}$, with one end converging asymptotically to the CMC cylinder C_λ and the other being a graph outside a compact set. Moreover, Σ_1 self-intersects, while Σ_2 and Σ_3 have monotonous height and in particular are embedded.

2. Case $1/2 < \lambda < 1$. In this case, the structure of Θ_1 and Θ_{-1} is shown in Figure 8 top left and right respectively. There are also three kind of orbits $\gamma_1(s), \gamma_2(s), \gamma_3(s)$ in Θ_1, and $\gamma_1(s)$ and $\gamma_3(s)$ behave as shown in Figure 10. The only difference here is that the orbit $\gamma_2(s)$ intersects

the line $y = -1$ at a finite point as s decreases. Then, $\gamma_2(s)$ enters to Θ_{-1} and converges to the line $y = y_0^-$ as $s \to -\infty$.

The corresponding $\mathfrak{h}_\lambda$-surfaces are also similar to the ones constructed in the previous case.

3. Case $\lambda \leq 1/2$. In this case, the structure of Θ_1 and Θ_{-1} is shown in Figure 8 bottom left and right respectively. In particular, no equilibrium point exists and the behavior of the orbits is different from the previous cases.

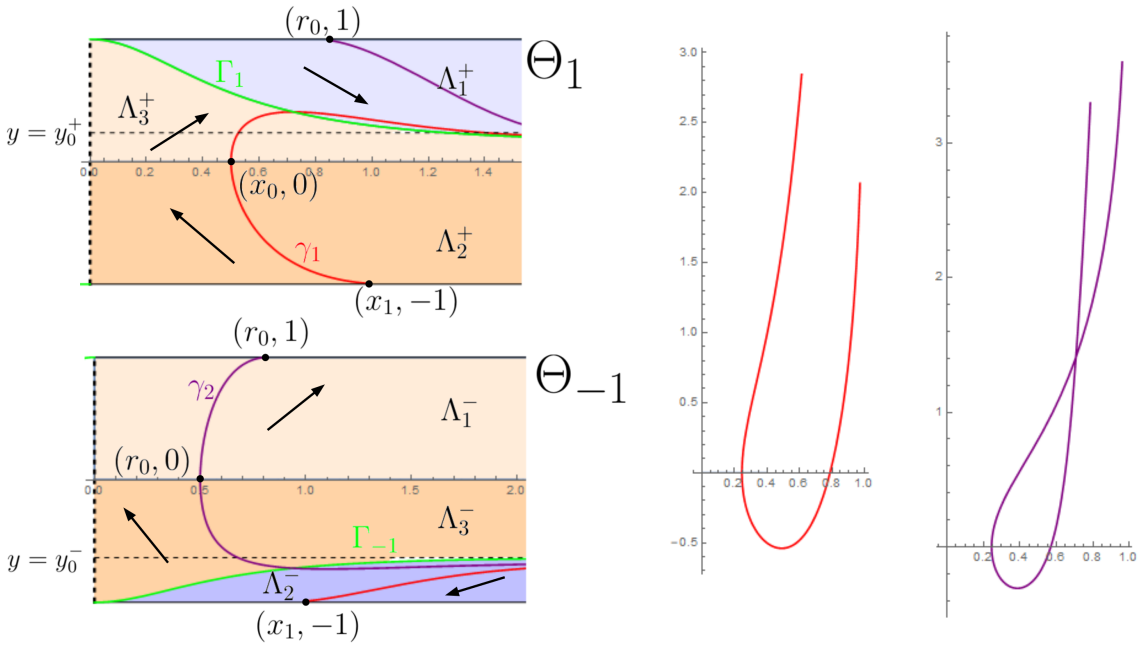

Figure 11: Left: the phase planes Θ_1 and Θ_{-1} for $\lambda = 1/3$ and the two types of orbits. Right: the profile curve of the corresponding rotational $\mathfrak{h}_\lambda$-surfaces for $\lambda = 1/3$.

First, let be $x_0 > 0$ and $\gamma_1(s)$ the orbit in Θ_1 such that $\gamma_1(0) = (x_0, 0)$. For $s > 0$, $\gamma_1(s)$ enters to Λ_3^+, intersects Γ_1 and then lies in Λ_1^+ converging to the line $y = y_0^+$. For $s < 0$, the orbit $\gamma_1(s)$ lies in Λ_2^+ and has some $\gamma_1(s_0) = (x_1, -1)$ as endpoint. Thus, $\gamma_1(s)$ for $s < s_0$ lies in Λ_2^- and stays there converging to the line $y = y_0^-$ as $s \to -\infty$. See Figure 11, the orbit in red.

Lastly, let be $r_0 > 0$ and $\gamma_2(s)$ the orbit in Θ_{-1} such that $\gamma_2(0) = (r_0, 0)$. For $s < 0$, $\gamma_2(s)$ enters the region Λ_3^- and ends up converging to the line $y = y_0^-$ as $s \to -\infty$. For $s > 0$, $\gamma(s)$ enters the region Λ_1^- and has as endpoint some $\gamma_2(s_0) = (r_1, 1)$. Then, $\gamma_2(s)$ for $s > s_0$ lies in Λ_1^+ and stays there as it converges to the line $y = y_0^+$ as $s \to \infty$. See Figure 11, the orbit in purple.

Again, we have two distinct $\mathfrak{h}_\lambda$-surfaces Σ_1 and Σ_2 generated by the orbits γ_1 and γ_2. Each Σ_i is properly immersed and diffeomorphic to $\mathbb{S}^1 \times \mathbb{R}$, and both ends are graphs outside compact sets. Moreover, Σ_1 is embedded, while Σ_2 self intersects; see Figure 11, right.

□

References

[AbRo] U. Abresch, H. Rosenberg, A Hopf differential for constant mean curvature surfaces in $\mathbb{S}^2 \times \mathbb{R}$ and $\mathbb{H}^2 \times \mathbb{R}$, *Acta Math.* **193** (2004), 141–174.

[AEG] J. A. Aledo, J. M. Espinar, J. A. Gálvez, Height estimates for surfaces with positive constant mean curvature in $\mathbb{M}^2 \times \mathbb{R}$, *Illinois J. Math.* **52** (2008), 203–211.

[Ale] A.D. Alexandrov, Uniqueness theorems for surfaces in the large, I, *Vestnik Leningrad Univ.* **11** (1956), 5–17. (English translation): Amer. Math. Soc. Transl. **21** (1962), 341–354.

[ADL] J. C. Artés, F. Dumortier, J. Llibre. Qualitative theory of planar differential systems. *Universitext. Springer-Verlag*, Berlin, 2006.

[BCMR] V. Bayle, A. Cañete, F. Morgan, C. Rosales, On the isoperimetric problem in Euclidean space with density, *Calc. Var. Partial Diff. Equations* **31** (2008), 27–46.

[BeEa] P. Berard, R. Sa Earp, Examples of H-hypersurfaces in $\mathbb{H}^n \times \mathbb{R}$ and geometric applications, *Mat. Contemp.* **34** (2008), 19–51.

[Bue1] A. Bueno, Translating solitons of the mean curvature flow in the space $\mathbb{H}^2 \times \mathbb{R}$, *J. Geom.* **109** (2018).

[Bue2] A. Bueno, Uniqueness of the translating bowl in $\mathbb{H}^2 \times \mathbb{R}$ *J. Geom.*, **111** (2020).

[Bue3] A. Bueno, The Björling problem for prescribed mean curvature surfaces in $\mathbb{R}^3$, *Ann. Global. Anal. Geom.* **56** (2019), 87-96.

[Bue4] A. Bueno, Half-space theorems for properly immersed surfaces in $\mathbb{R}^3$ with prescribed mean curvature, *Ann. Mat. Pura. Appl.* **199** (2020), 425–444.

[Bue5] A. Bueno, A Delaunay-type classification result for prescribed mean curvature surfaces in $\mathbb{M}^2(\kappa) \times \mathbb{R}$, *Pacific. J. Math.* (2021), to appear.

[Bue6] A. Bueno, Properly embedded surfaces with prescribed mean curvature in $\mathbb{H}^2 \times \mathbb{R}$, *Ann. Global. Anal. Geom.* **59** (2021), 69–80.

[BGM1] A. Bueno, J.A. Gálvez, P. Mira, The global geometry of surfaces with prescribed mean curvature in $\mathbb{R}^3$, *Trans. Amer. Math. Soc.* **373** (2020), 4437-4467.

[BGM2] A. Bueno, J.A. Gálvez, P. Mira, Rotational hypersurfaces of prescribed mean curvature, *J. Differential Equations* **268** (2020), 2394–2413.

[BuOr] A. Bueno, I. Ortiz, Invariant hypersurfaces with linear prescribed mean curvature, *J. Math. Anal. Appl.* **487** (2020), 124033.

[Chr] E.B. Christoffel, Über die Bestimmung der Gestalt einer krummen Oberfläche durch lokale Messungen auf derselben. *J. Reine Angew. Math.* **64** (1865), 193–209.

[GaMi1] J.A. Gálvez, P. Mira, Uniqueness of immersed spheres in three-manifolds, *J. Differential Geometry* **116** (2020), 459–480.

[GaMi2] J.A. Gálvez, P. Mira, Rotational symmetry of Weingarten spheres in homogeneous three-manifolds *J. Reine Angew. Math.* **773** (2021), 21–66.

[GuGu] B. Guan, P. Guan, Convex hypersurfaces of prescribed curvatures, *Ann. Math.* **156** (2002), 655–673.

[Ilm] T. Ilmanen, Elliptic regularization and partial regularity for motion by mean curvature, *Mem. Amer. Math. Soc.* **108** (1994).

[LiMa] J. H. S. de Lira, F. Martin, Translating solitons in Riemannian products, *J. Differential Equations* **266** (2019), 7780–7812.

[Lop] R. López, Invariant surfaces in Euclidean space with a log-linear density, *Adv. Math.* **339** (2018), 285–309.

[Min] H. Minkowski, Volumen und Oberfläche, *Math. Ann.* **57** (1903), 447–495.

[Oni] I. I. Onnis, Invariant surfaces with constant mean curvature in $\mathbb{H}^2 \times \mathbb{R}$, *Ann. Mat. Pura. Appl.* **187** (2008), 667–682.

[Pip1] G. Pipoli, Invariant translators of the Heisenberg group, *J. Geom. Anal.* **31** (2021), 5219–5258.

[Pip2] G. Pipoli, Invariant translators of the Solvable group, *Ann. Mat. Pura. Appl.* **199** (2020), 1961–1978.

[Pog] A.V. Pogorelov, Extension of a general uniqueness theorem of A.D. Aleksandrov to the case of nonanalytic surfaces (in Russian), *Doklady Akad. Nauk SSSR* **62** (1948), 297–299.

The author was partially supported by P18-FR-4049.